nanda, Proc. Phys. Soc. (London) 87, 917 (1966).
[28]M. E. Rose, Phys. Rev. 91, 610 (1953).
[29]M. L. Narasimha Raju, V. Seshagiri Rao, and D. L. Sastry, Phys. Rev. C 2, 566 (1970).
[30]R. M. Singru, P. C. Simms, and R. M. Steffen, Phys. Rev. 141, 1078 (1965).
[31]M. L. Narasimha Raju, V. Seshagiri Rao, and D. L. Sastry, Indian J. Pure App. Phys. 9, 308 (1971).
[32]C. W. E. Van Eijk, Nucl. Phys. A169, 239 (1971).

PHYSICAL REVIEW C VOLUME 7, NUMBER 3 MARCH 1973

Prompt Gamma Rays from ^{235}U(n,f), ^{239}Pu(n,f), and Spontaneous Fission of ^{252}Cf†

V. V. Verbinski, Hans Weber, and R. E. Sund
Intelcom/Rad Tech, P. O. Box 80817, San Diego, California 92138

(Received 28 July 1972)

The spectra of prompt γ rays from ^{235}U(n,f), ^{239}Pu(n,f), and ^{252}Cf(s.f.) emitted at 0–10 nsec after fission were measured with <4-nsec time resolution. A γ-ray spectrometer with a near-Gaussian response was used over the entire energy region, and the prompt neutrons from fission were positively rejected by time of flight. The measured γ-ray spectra show a systematic softening with increasing mass number for ^{235}U, ^{239}Pu, and ^{252}Cf. The average photon energy above 0.14 MeV is 0.97 ± 0.05, 0.94 ± 0.05, and 0.88 ± 0.04 MeV/photon for thermal-neutron fission of ^{235}U and ^{239}Pu, and spontaneous fission of ^{252}Cf, respectively. This behavior is discussed in terms of nearness of Z and N of the average fission fragment to closed-shell values, of the corresponding changes in level density expected, and of corroborative evidence from x-ray measurements. The total γ-ray energy released, $\bar{E}_{\gamma,\mathrm{tot}}$, is 6.51, 6.81, and 6.84 MeV/fission for ^{235}U(n,f), ^{239}Pu(n,f), and ^{252}Cf (s.f.), respectively, for photons above 0.14 MeV and for 0–10 nsec after fission. The calculations of Thomas and Grover are seen to be in agreement with these data in that they predict the correct partition of fission-fragment deexcitation energy between neutron and photon emission. This partition is related to the separation energy required to emit an additional neutron, to the pairing energy, and to the spin barrier for neutron emission. Two theoretical γ-ray spectra were compared to the measured spectrum for ^{235}U(n,f), and each was found to fit the measured spectrum well over only a limited portion of the total energy range.

I. INTRODUCTION

The γ-ray energy spectrum per fission event was measured for thermal-neutron fission of ^{235}U and ^{239}Pu and for spontaneous fission of ^{252}Cf with the same apparatus and techniques so that meaningful comparisons between the three could be made. Most systematic errors are the same for all three cases so that small differences in the results for the three fission species can be observed. In addition, the measurements were carried out with techniques which add significantly to the absolute accuracy and reliability of the results. These include the time-of-flight separation of the prompt-neutron-induced background counts in the detector, the use of a single spectrometer with a nearly Gaussian response over the entire energy range, and the use of fast-timing circuitry for measuring γ rays in prompt coincidence with the fission event.

The physical parameters derived from these measurements that are of interest for comparison with theory are the spectral shape $\vec{\varphi}(E_\gamma)$, the total average energy $E_{\gamma,\mathrm{tot}}$ carried off in the process of deexciting the fission fragments, and the average number of γ rays emitted, or, alternatively, their average energy $E_{\gamma,\mathrm{av}}$. Variations of spectral shape and of the quantities $E_{\gamma,\mathrm{tot}}$ and $E_{\gamma,\mathrm{av}}$ versus (i) the initial excitation energy of both fission fragments, (ii) the mass of the fission species, and (iii) the initial spin of the fissionable nucleus are of primary interest. The historical development of the calculations of these quantities is briefly outlined below.

The calculations of γ rays accompanying fission include all photons emitted before the neutron-emission cascade has been completed and all γ rays following the neutron cascade but preceding β decay of the fragment. These include isomeric γ rays preceding β decay; these isomeric γ rays are considerably more intense than the γ rays following β decay for times less than $\sim10^{-3}$ sec. Most of the photon emission occurs after all of the neutrons have been emitted. Zommer, Saveliev, and Prokofiev[1] derived an upper limit of only ~4% for the fraction of γ-ray energy emitted before the

last neutron is given off. After neutron emission, ~80% of the photon energy is emitted with γ rays having half-lives of 10^{-11} sec or less and ~15% with half-lives of 10^{-9}–10^{-10} sec.[2] The measurements presented here were made in prompt coincidence (10^{-8} sec) with the fission event and include the subnanosecond γ rays plus a small amount of the longer-lived "isomeric" γ rays above the 140-keV bias for this experiment. Since this region of decay time and γ-ray energy constitutes ~97% of all the fission-fragment deexcitation γ-ray energy preceding β decay,[3-5] these results can be compared directly to the calculations of spectral shape, $E_{\gamma,\mathrm{tot}}$ and $E_{\gamma,\mathrm{av}}$ discussed below.

A number of early calculations of prompt γ-ray energy that can be found in the literature[6-9] yielded $\bar{E}_{\gamma,\mathrm{tot}}$ of about half the average neutron binding energy $\bar{E}_b$ for each of the two fission fragments, or

$$E_{\gamma,\mathrm{tot}} \approx \bar{E}_b \leq 5 \text{ MeV}. \quad (1)$$

Zommer, Saveliev, and Prokofiev[1] carried out a statistical theory calculation for $^{235}\mathrm{U}(n,f)$ that included a γ-ray spectrum prediction as well as $E_{\gamma,\mathrm{tot}}$. With a better value for $\bar{E}_b$ and with an upper-limit estimate of 0.3 MeV for pre-neutron-emission γ rays, they obtain

$$E_{\gamma,\mathrm{tot}} \leq 0.95\bar{E}_b + 0.3 = 6.2 \text{ MeV/fission} \quad (2)$$

and indicate that if their calculations could have taken into account the wide spacing of nuclear levels near ground state, and the high angular momentum of the fission fragments, their calculated value of $E_{\gamma,\mathrm{tot}}$ would have been higher than this upper limit of 6.2 MeV/fission.

Gordon and Aras[10] have included an explicit pairing-energy correction for level densities in a Monte Carlo type calculation, obtaining

$$E_{\gamma,\mathrm{tot}} \cong \bar{E}_b + \delta, \quad (3)$$

where δ is the pairing-energy correction. They obtain $E_{\gamma,\mathrm{tot}} = 7.66$ MeV in this way, and $E_{\gamma,\mathrm{tot}} = 5.03$ MeV with all δ values set equal to zero. The assumption of no neutron emissions after the neutrons deexcite the fission fragment to an energy below $(\bar{E}_b + \delta)$ may be unrealistic, however, as discussed in Sec. VII.

Grover and Nagle[11] have shown that neutron-unstable nuclei with spins greater than $\frac{7}{2}$, and which can decay only to a spin-zero level, decay preferentially by γ-ray emission even though the neutrons could decay with energies of several hundred keV. The subsequent calculations of Thomas and Grover[12] took into account the high angular momentum of fission fragments (the angular momentum barrier for neutron emission), as well as the pairing energy. The latter was taken into account implicitly in these calculations, so that the relationship of the computed value of $E_{\gamma,\mathrm{tot}}$ to $\bar{E}_b$ and to the pairing energy cannot be determined as directly as in the calculations of Gordon and Aras. Nevertheless, the Thomas and Grover calculations are the more comprehensive and the most useful as will be discussed further in Sec. VII A.

The photon spectrum $\vec{\varphi}(E_\gamma)$ was obtained by Thomas and Grover[13] in the course of carrying out their calculations.[12] Both their predictions and those of Zommer, Saveliev, and Prokofiev[1] for $E_{\gamma,\mathrm{tot}}$ as well as the spectral shape $\vec{\varphi}(E_\gamma)$, are compared with experimental results in Sec. VII.

II. EXPERIMENTAL METHOD AND APPARATUS

A. Method

The basic experimental arrangement, shown schematically in Fig. 1, employed a thin sample of fissionable material placed next to a fission-fragment detector and 70 cm from a NaI crystal γ-ray spectrometer surrounded by a NaI anti-Compton sheath. The fissionable material was irradiated with a thermal-neutron beam during the measurements with $^{235}\mathrm{U}$ and $^{239}\mathrm{Pu}$, and the beam was simply shut off for the $^{252}\mathrm{Cf}$(s.f.) measurements. The experimental arrangement was thus kept nearly identical for all three measurements.

The surface-barrier detector provided a zero-time reference for the fission events, and the γ-ray spectrometer counts were measured within 10 nsec of fission with <4-nsec time resolution. The 70-cm separation of the fissionable material and γ-ray spectrometer resulted in about a 15-nsec traversal time for 10-MeV neutrons. Consequently, practically all of the interfering events from the prompt fission neutrons were eliminated by time-of-flight separation; alternative methods of correcting for the prompt neutrons are much less accurate. Figure 2 shows the excellent separation of prompt-γ-ray and neutron events for $^{252}\mathrm{Cf}$(s.f.). The time resolution of our coincidence system is seen to be less than 4 nsec full width at half maximum. The area under the neutron peak is about 28% for $^{252}\mathrm{Cf}$(s.f.), and 17% for $^{235}\mathrm{U}(n,f)$, being approximately proportional to the number of prompt neutrons per fission, $\bar{\nu}_p$, for each species. This is about the magnitude of the prompt-neutron background correction that would have to be made for this spectrometer if time-of-flight separation had not been achieved. Without time-of-flight separation, the differences in $\bar{\nu}_p$ for the different fission species would clearly mask the

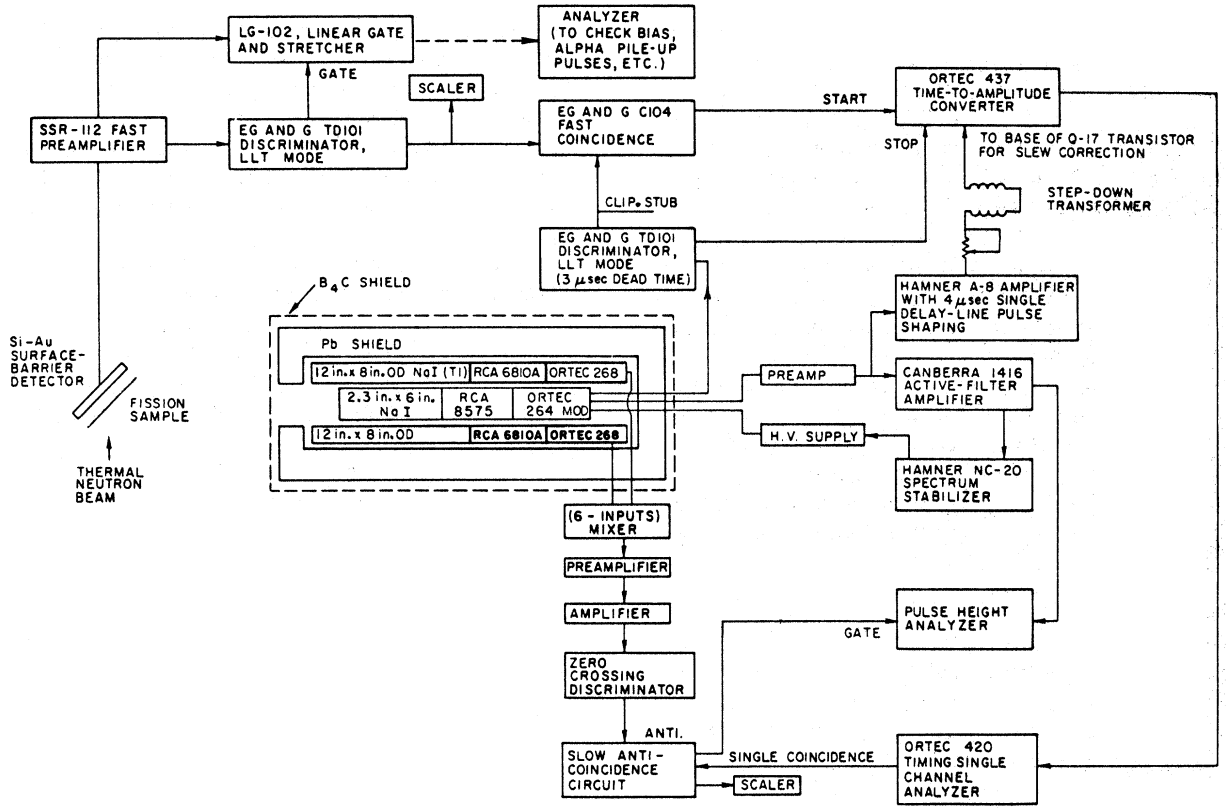

FIG. 1. Block diagram of experimental setup and electronics.

small differences in photon yields measured for the three cases.

Backgrounds due to chance coincidence events were measured well before the prompt-γ-ray peak of Fig. 2, and were subsequently subtracted.

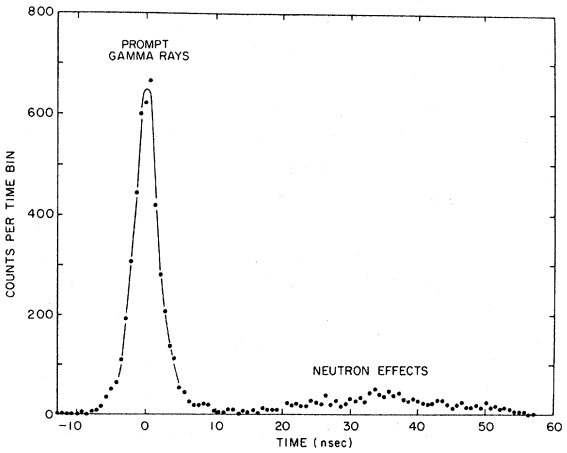

FIG. 2. Intensity of γ-ray events observed with the present spectrometer as a function of time after the detection of ^{252}Cf fission fragments. The results show <4-nsec resolution.

The γ-ray spectrometer with a Compton-scattering anticoincidence sheath produces a highly localized response consisting of a main near-Gaussian peak with a greatly reduced Compton-scattering tail (see Fig. 3). The localized response, and also the use of a single spectrometer to cover the entire energy range of 0.14 to 10 MeV, are of utmost importance in reducing spectrum-unscrambling errors discussed further below.

B. Experimental Geometry

The neutrons that irradiated the ^{235}U and ^{239}Pu fission foils arrived from a 15-cm-diam disk source at the face of a graphite thermal-neutron column 10 m away. This beam was well collimated and highly thermalized, yielding a cadmium ratio for ^{235}U of about 350. The neutrons irradiated 10-cm^2 targets of ^{235}U or ^{239}Pu which were ~200 μg/cm^2 thick, >99.7% enriched, and deposited on 5×10^{-4}-cm-thick stainless-steel substrates. A 9.5-cm^2 ORTEC heavy-ion fission-fragment detector was located 0.25 cm from the fission foil; this small separation reduced the spread in fission-fragment time of flight to an acceptably low value.

The wide acceptance angle of the fission-fragment detector, the 200-$\mu g/cm^2$ foil thickness of ^{235}U, and the fast preamplifier used produced the broad pulse-height distribution as shown in Fig. 4; however, all the fission-fragment events are safely above the detector bias shown in the figure. The effects of deterioration of the fission-fragment detector by radiation damage were reduced to a reasonably low level by cooling the detectors to −30°C and replacing them when necessary.

The nonisotropic angular distribution of γ rays with respect to the direction of the fission-fragment trajectories[14,15] can also introduce an error in the measurements. Calculations on the magnitude of these effects showed them to be negligible for the conditions of the present experiment, i.e., for the 0.25-cm source-detector separation, and with the normal to the fission-foil plane placed about 60° to the line joining the foil and the γ-ray spectrometer.

The NaI γ-ray spectrometer consisted of a 5.85-cm-diam by 15.2-cm-long NaI(Tl) crystal located at the center of a 20.3-cm outside diameter by 30.5-cm-long NaI(Tl) annulus. The annulus was well shielded with lead and boron, and a thin layer of $^{10}B_4C$ (95% ^{10}B enrichment) was placed between the center crystal and fission foil to reduce thermal-neutron background counts to an acceptably low level.

C. Electronics

Figure 1 shows the block diagram of the electronics used to achieve the fast timing and reproducible γ-ray response matrix necessary for the low background and accurate spectrum unfolding. The fast signals from the center detector were accepted if they occurred within 10 nsec of the timing pulses from the fission-fragment detector. The time slewing of the NaI detector was reduced considerably by a method of slew correction[16] in which a portion of the linear signal from the single delay-line amplifier (see Fig. 1) was added to the time-to-amplitude converter (TAC) output; the gain of this amplifier was adjusted to obtain saturating pulses at higher pulse heights, where no time-slewing correction was required. The TAC start and stop signals were obtained from the fission-fragment detector and γ-ray spectrometer as shown in Fig. 1. Pulses from −10 to +10 nsec were accepted in the measurements (see Fig. 2). A spectrum stabilizer circuit kept the gain of the analyzed pulses constant. The gain stability and linearity of an ORTEC model-264 photomultiplier base with the RCA-8575 photomultiplier tube had to be improved for these experiments. This was

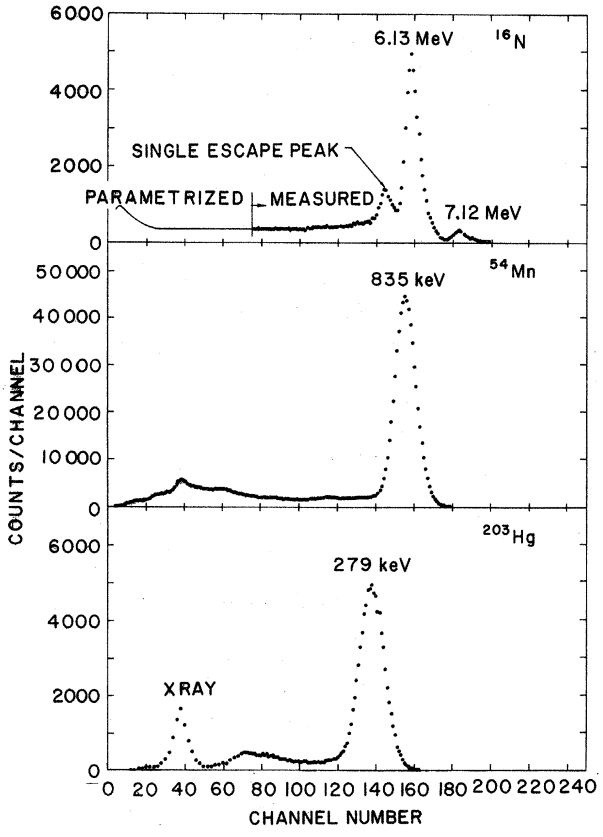

FIG. 3. Typical raw NaI pulse-height distributions used to parametrize the response functions. The ^{16}N data below ~2.75 MeV show the results after the ^{24}Na γ rays were subtracted.

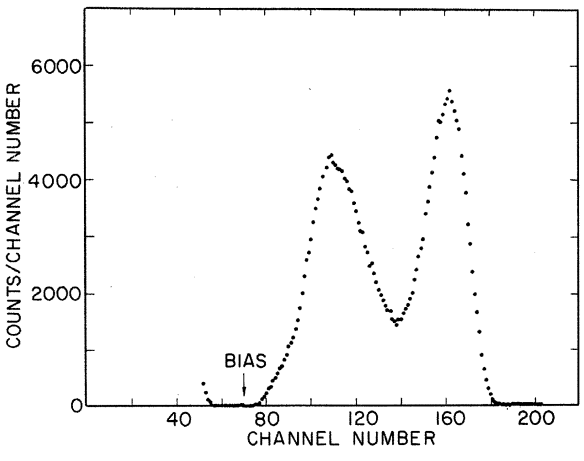

FIG. 4. Pulse-height spectrum of ^{235}U fission fragments with uncollimated detector 0.25 cm from fission foil. The discriminator bias was always below the height of the smallest fission-fragment pulse.

achieved with additional stabilizing capacitors from ground to a previously unstabilized dynode and focus grid, and with reducing the voltage-divider resistors by a factor of 3. The response functions for the spectrometer were kept constant by operating the anti-Compton NaI(Tl) sheath at a low pulse-height bias of about 35 keV, where small changes of bias produced very minor changes in the suppressed Compton tail. At biases well above 50 keV, the sensitivity to bias change was unacceptably high. The NaI sheath was also important in eliminating single and double escape peaks from pair production.

D. Background Problems

With the time-of-flight elimination of the dominant source of background, that due to prompt-fission-neutron counts, the remaining source is due to chance coincidence events. These can be seen to the left of the prompt-γ-ray peak in the time distribution of Fig. 2. The rate was one count per 2000 true coincidences for ^{252}Cf and one per 200 for the ^{235}U and ^{239}Pu measurements. This background was disproportionately large at high γ-ray energies due to the thermal-neutron capture events in the material surrounding the fission foil, and careful subtraction was required to obtain good accuracy above ~6 MeV for the ^{235}U and ^{239}Pu cases where the thermal neutron beam was turned on. The chance coincidence background was about 10% of the total counts in the 5.5–6.5-MeV region and about 40% in the 6.5-7.5-MeV region.

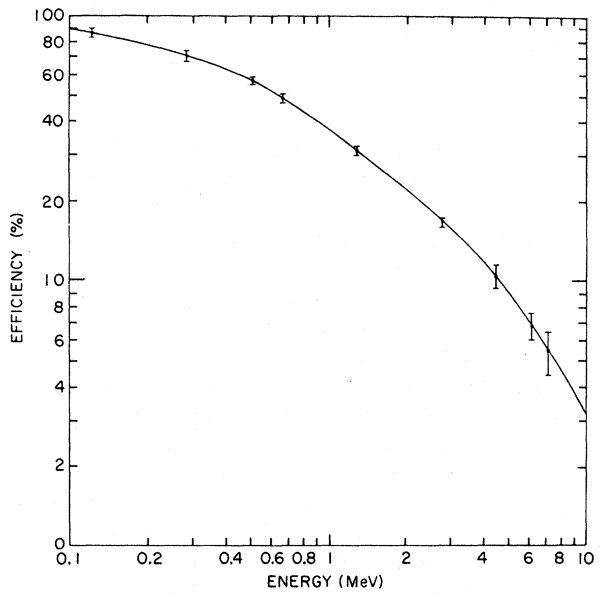

FIG. 5. Absolute photopeak efficiency of the NaI spectrometer for detecting γ-ray events. The effect of the present experimental geometry is included in these data.

E. Detector Calibration

To obtain energy spectra, the measured pulse-height distributions had to be unfolded with the use of a matrix equation presented below. As input for each unfolding operation, a response matrix consisting of 200 response vectors for monoenergetic γ rays was required. These vectors were obtained from calibrations with the following γ-ray sources with energies in MeV in parentheses; ^{57}Co (0.122), ^{203}Hg (0.279), ^{22}Na (0.511, 1.275), ^{137}Cs (0.662), ^{54}Mn (0.835), ^{88}Y (0.90, 1.84), ^{24}Na (1.37, 2.75), PuBe (4.44) with the use of paraffin and lead shields, and ^{16}N (6.13, 7.12). Three spectra are shown in Fig. 3. When a source had two γ rays, the catalog of response vectors was built up as composites with proper subtraction techniques. For example, a ^{22}Na source gave an excellent 1.275-MeV γ-ray response vector for energies above the 0.511-MeV ^{22}Na positron-decay γ rays. Below 0.511 MeV, the shape of the Compton edge and source-backscatter peaks was obtained with adequate accuracy from the two ^{60}Co γ rays near 1.275 MeV. The ^{16}N data of Fig. 3 show some γ rays at 7.12 and 6.13 MeV. Below ~2.75 MeV, some ^{24}Na γ rays were present; the parametrized ^{24}Na responses were utilized to subtract these γ rays from the raw data and obtain the ^{16}N responses shown. The response vectors were fitted with analytic functions at all the available experiment energies, and these functions were then used to represent the 200 responses required to construct the response matrix. The accuracy of the fit was tested at many energies with both single and composite γ-ray lines, and with sources of known intensity.

The efficiency versus energy for the total energy peak, often called the photopeak, is shown in Fig. 5 for our 5.85-cm-diam × 15.2-cm-long NaI detector. The photopeak efficiency versus γ-ray energy was obtained by three methods: (i) calibration up to 1.84 MeV with known standards obtained from several sources,[17] (ii) calibration at higher energies by means of sources such as ^{24}Na in which two or more γ-ray lines of known relative intensity are emitted, one of which has an energy low enough to fall into the lower energy region previously calibrated, and (iii) cross calibration at 4.44, 6.13, and 7.12 MeV against a standard size (5.48-cm-diam by 5.48-cm-long) NaI(Tl) detector calibrated by Jarczyk *et al.*[18] A cross check against Jarczyk's calibration with our independent method using the ^{24}Na 2.75- and 1.37-MeV lines gave an agreement well within the 3% error on this point quoted by Jarczyk *et al.* The error bars shown in Fig. 5 in-

clude the errors quoted by Jarczyk *et al.*, and the statistical and estimated systematic errors contributed by our cross-calibration procedure.

III. DATA AND ERROR ANALYSIS TECHNIQUES

A. General Description

The pulse-height distribution for all γ-ray events occurring within 10 nsec of fission were measured, and the chance coincidence background events were measured well before the prompt-γ-ray peak. The net prompt-γ-ray pulse-height distribution (pulse-height vector) $\vec{Y}$ and error vector $\vec{\Delta}$ were calculated and entered as inputs to the LSMUN spectrum-unfolding code described below. To improve the accuracy of the low-energy data, a 200-channel pulse-height vector $\vec{Y}$ was obtained for each of two gain settings, and a double-unfold method was devised to extend the range of the unfolding code to lower energies. The errors on the unfolded spectrum $\vec{\phi}$ were derived separately, as described below.

B. Unfolding Code

The response matrix $\bar{G}_{ij}$ was calculated with a response equation parametrized to fit calibration line spectra, as described in Sec. II E above. The energy mesh of the response vectors in each case corresponded to that of the input pulse-height data $\vec{Y}$ to be unfolded. The amplitude of each column vector $\vec{G}_i$ of $\bar{G}_{ij}$ for a monoenergetic source of energy E_j was properly normalized to the measured photopeak efficiencies (see Fig. 5).

The pulse-height distribution vector $\vec{Y}$ is related to the spectrum vector $\vec{\varphi}$ and the instrument response matrix $\bar{G}$ by

$$\vec{Y} = \bar{G}\vec{\varphi}\,. \tag{4}$$

However, the solution

$$\vec{\varphi} = \bar{G}^{-1}\vec{Y} \tag{5}$$

oscillates violently for most cases, and smoothing of some sort must be utilized.

The LSMUN[19] of Carl Young's code embodies the method of Cook[20] to accomplish this. Utilizing the calculus of variations, Eq. (4) takes the form

$$[\bar{G} + \lambda(\tilde{\bar{G}})^{-1}(\bar{W})^{-1}\bar{S}\,]\vec{\varphi} = \vec{Y}\,, \tag{6}$$

where $(\tilde{\bar{G}})^{-1}$ is the inverse of the transposed $\bar{G}$ matrix, $\bar{S}$ is a smoothing matrix determined by a structure function $S(\varphi)$ which is arbitrary within limits and is usually chosen as a function of the slope or the curvature of the solution $\vec{\varphi}$, and λ is a Lagrangian multiplier. $\bar{W}$ is a diagonal matrix with elements $W_{ii} = (1/\Delta y_i)^2$ and thus contains weighting factors which become small in the vicinity of a γ-ray peak in φ_j, so that the smoothing in this region is nearly turned off. The Δy_i are the 200 components of the input error vector Δ_i which represent the standard deviation of the input pulse-height distribution y_i.

An initial value of λ is used as an input to LSMUN, and the code is then used to obtain a solution to Eq. (6) for $\vec{\varphi}$. This solution is then multiplied by $\bar{G}$, as in Eq. (4), and the energy spectrum $\vec{\varphi}$ is thus refolded to get the precise value of $\vec{Y}$ (refold) that corresponds to the initial solution $\vec{\varphi}$. A χ^2 test is performed utilizing the difference $(\bar{y}_i - y_i)$ where $\bar{y}_i$ corresponds to the refold of the solution $\vec{\varphi}$, and y_i to the input raw data in channel i. The value of λ is varied in an iterative manner until the value of χ^2 approximately equals N, where N is the number of channels of the input data, or alternatively the dimension of the data vector $\vec{Y}$.

The LSMUN code was tested for self-consistency by determining the accuracy with which it could unfold pulse-height distributions for single- and multiple-line γ-ray sources of known source strength. The code was found to be self-consistent at all energies within a few percent and the error indicated in the self-consistency test was always reasonable with respect to the error bars on the efficiencies. At low channels, where the full width at half maximum of the photopeak was less than two channels wide, the LSMUN code produced normalization factor errors. These were computed, and the corresponding correction factors were applied to the code. However, these were mostly circumvented by a double-unfolding technique we used.

C. Double Unfolding

The code normally covered the range from 0.3 to 10 MeV, whereas the lower energy limit of the NaI pulse-height distribution was 0.07 MeV, as determined by the discrimination setting for the center detector. To overcome the resolution limit of the unfolding code at the low-energy end and to extend the range to lower energies, we made use of an additional high-gain (low-energy) run and double-unfolded the data. This low-energy unfolding was accomplished by first unfolding the high-energy data to obtain $\vec{\varphi}$ (0.3 → 10 MeV), and then folding back in $\vec{\varphi}$ (1 → 10 MeV) by having Eq. (4) operate on the spectrum above 1 MeV. This folded-in pulse-height distribution was then subtracted from the high-gain (low-energy) raw data, yielding the NaI pulse-height distribution that would have resulted if all γ rays above 1 MeV had been absent. The net high-gain pulse-height distribution (below 1 MeV), along with the correct stan-

dard deviations resulting from the Compton-tail subtractions for γ rays above 1 MeV, was then used as input to the LSMUN code which provided $\vec{\varphi}(E)$ with good energy resolution and reasonable accuracy down to 140 keV. Below this, the energy spectrum was seen to drop rapidly for these very prompt γ rays, and the unfolding accuracy rapidly deteriorated because of the rapid accumulation of "Compton-tail subtraction" errors. This accounts for our low-energy cut off of 140 keV.

To eliminate any oscillations in the unfolded results at low energies, the unfolding was done with a reduced photopeak width in the response matrix as compared to the actual experimental width without altering the photopeak efficiency. The resolution of the peak-like structure is slightly reduced with negligible effect on the values for the energy per fission and the number of γ rays per fission. This method of reducing oscillations is somewhat akin to that first proposed by Brunfelter, Kockum, and Zetterström.[21]

D. Experimental Errors

The most important sources of experimental errors were counting statistics, detector-efficiency calibration, generation of the response-matrix, and unfolding the data.

The nearly singular response functions of our detector and the rapidly falling spectrum with increasing energy facilitated a reasonably straightforward calculation of the statistical error for the unfolded spectrum, $\vec{\varphi}(E_\gamma)$. The fractional error on $\vec{\varphi}(E_\gamma)$ for each channel k was obtained by first adding in quadrature the errors from the following two quantities: (1) the raw data counts y_k in channel k and (2) the Compton-tail plus escape-peak counts y_k'' in channel k that are due to photons for energy greater than E_k. The square root of this quantity divided by the "photopeak counts" y_k' gives the fractional error in the "photopeak counts," or equivalently, the fractional error in $\vec{\varphi}(E_\gamma)$ for each channel k. The value of y_k' is simply $y_k - y_k''$, where y_k'' is obtained by refolding that part of the spectrum $\vec{\varphi}(E_\gamma)$ that lies above E_k.

To estimate the systematic errors associated with response-function inaccuracies, a typical low-gain spectrum was unfolded with the Compton-tail portion intentionally increased by 20%. This is considerably more than our fitting error for the response functions. The difference in the spectral shape $\vec{\varphi}(E_\gamma)$ caused by the 20% increase was less than the combined uncertainties due to counting statistics and detector-efficiency measurements. In addition, the total γ-ray energy per fission above 300 keV, $E_{\gamma,\mathrm{tot}}$ changed by only 2% for this test run. This insensitivity of $E_{\gamma,\mathrm{tot}}$ to fractional changes in the Compton tail indicates that any reasonable errors in our measurements of the response functions and the subsequent parametrization of these functions did not contribute significantly to the over-all error in $\vec{\varphi}(E_\gamma)$, $E_{\gamma,\mathrm{tot}}$, and $E_{\gamma,\mathrm{av}}$.

Coding errors were found at low channel numbers due to finite channel widths, as mentioned at the end of Sec. III B, but the appropriate corrections were calculated in each case. This source of error was thus reduced to a relatively insignificant amount. The accuracy of the unfolding code was always checked by carrying out the refold of $\vec{\varphi}(E)$ according to Eq. (1). This refold was accurate because it utilized the direct response matrix $\overline{G}$ without the conditioning terms used in the unfolding matrix of Eq. (6). Thus, it is reasonably certain that the dominant error on the spectrum arises from detector-efficiency calibration, except above 5 or 6 MeV, where $\vec{\varphi}(E)$ is small and the statistical errors large. It then follows that the dominant error on the integrated quantities such as $E_{\gamma,\mathrm{tot}}$ is also limited by the accuracy of the detector efficiency calibration. The upper limit of the efficiency effects on the measured value of $E_{\gamma,\mathrm{tot}}$ are about ±3%. A conservative over-all error of 5% is suggested, or about ±0.3 MeV on $E_{\gamma,\mathrm{tot}}$ for energies above 0.140 MeV and emission times of 0–10 nsec after fission.

IV. RESULTS

In Fig. 6 is shown the NaI pulse-height distribution for prompt γ rays from thermal-neutron fission of ^{235}U, and below it the unfolded energy spectrum of γ rays per fission event. At high energies the data have been grouped, as indicated by the spacing of the points in the figure. Below 0.7 MeV, the high-gain (low-energy) NaI data and the results of the double unfolding are shown. The high-gain raw data agreed well with the low-gain data in the overlap region of 0.2 to 1.0 MeV, with both sets of data normalized to the same number of fission events and the energy width of the analyzer channel. This good agreement was important in obtaining accurate spectra and good reproducibility. The unfolded data were similarly checked in the overlap region and were found to agree well. The same structure that appears in the pulse-height distribution $\vec{Y}$ below 1 MeV can also be seen in the unfolded energy spectrum $\vec{\varphi}(E_\gamma)$ shown in Fig. 6. Because the response function is nearly localized, the slope at the unfolded data essentially agrees with the raw data, except for the efficiency versus energy. This similarity indicates that there is little error propagated in the unfolding process. In fact, most of the difference in the shape of the two

curves is simply due to the shape of the efficiency curve $\epsilon(E)$. At all points on the pulse-height distribution where the slope is negative and steep, $\vec{\varphi}(E)$ is only slightly less than $y_i/\epsilon(E)$, where i is proportional to E. This is because the Compton and pair events from higher-energy γ rays are relatively weak in intensity, since they are suppressed by the spectrometer. At high energies the unfolded data appear smoother than the pulse-height distribution because of the smoothing routine in the unfolding code, as explained in Sec. III B above. The error bars shown in the figure on the raw data, as well as the unfolded data, represent only the statistical uncertainties. In addition, there are systematic errors which are mostly due to the efficiency calibration of the γ-ray detector, as discussed above (see Fig. 5).

Figures 7 and 8 show γ-ray pulse-height distributions and unfolded spectra for ^{239}Pu(n,f) and ^{252}Cf-(s.f.). A comparison of our results for ^{235}U(n,f), ^{239}Pu(n,f), and ^{252}Cf(s.f.) is given in Fig. 9.

In Table I the energy emitted per fission event in the form of prompt-γ radiation and the number of γ rays per fission are given for a number of energy intervals above 0.14 MeV; the over-all errors are given in the caption, and the statistical errors for the partial results are presented in Figs. 6–8.

The data of Table I lead to values of 0.97 ± 0.05, 0.94 ± 0.05, and 0.88 ± 0.04 MeV/photon for γ rays above 0.14 MeV emitted within less than 10 nsec after fission of ^{235}U, ^{239}Pu, and ^{252}Cf, respectively. The errors include over-all systematic errors. The relative errors that enter in comparing the results between the three different fission species are estimated to be about one third as large.

V. OTHER MEASUREMENTS

No previous measurements have been published on prompt-γ rays from ^{239}Pu(n,f). The earliest work of note on ^{235}U(n,f) was the work of Peelle and Maienschein[5] that postdates their early preliminary results[22] that first appeared in 1958 and are still sometimes found to be in use. Our results, which appeared first in informal report form in 1969,[23] agree well in spectral shape with their latest 1971 results,[5] as presented in Fig. 6 of their article, even though we used a single NaI(Tl) spectrometer with anti-Compton sheath and they used a single-crystal, a Compton-, and a pair-spectrometer to cover the range of 0.01–10

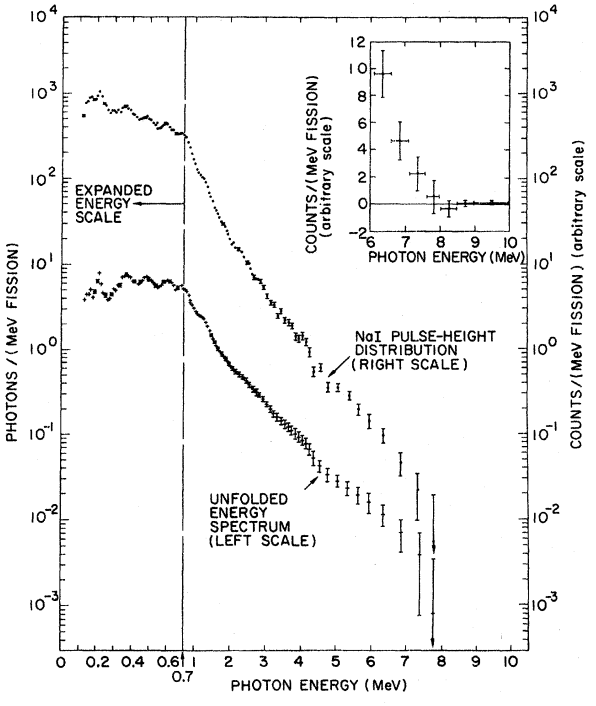

FIG. 6. NaI pulse-height distribution from the thermal-neutron fission of ^{235}U. The insert shows the data at high energies on a linear scale. Also shown is the unfolded spectrum. The difference between the shapes of the two curves is primarily due to the change in efficiency with energy. The error bars are too small to show in the 0.7- to 1.5-MeV region.

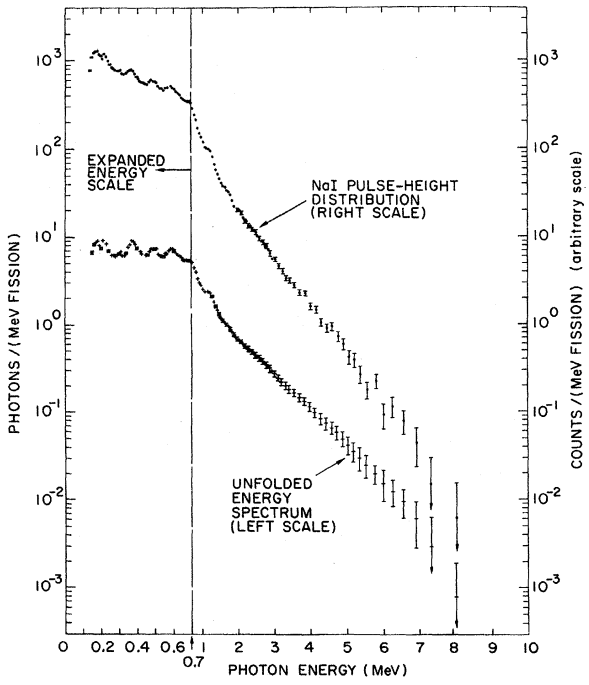

FIG. 7. NaI pulse-height distribution for prompt γ rays from the thermal-neutron fission of ^{239}Pu. Also shown is the unfolded spectrum. The error bars are too small to show in the 0.7- to 1.5-MeV region.

MeV. Both sets of data yield $E_{\gamma,av} = 0.97$ MeV/photon. Their value of $E_{\gamma,\,tot}$ for 0.14–10-MeV γ rays is 7.18 ± 0.26 MeV/fission for ≤69 nsec after fission. This compares with our value of 6.51 ± 0.3 MeV/fission for 0.14–10 MeV photons at 0–10 nsec after fission. Our recent measurements[3] on delayed γ rays from fission indicate that only about 0.05 MeV/fission of photon energy is emitted between 10 and 70 nsec after fission. This leaves a difference of 0.62 MeV/fission for $E_{\gamma,\,tot}$ as compared to 0.56 MeV/fissions for the combined error estimates, a reasonable agreement considering the difference in measuring times of about ten years and the difference in the measuring and data-unscrambling techniques. They used time-of-flight neutron separation at the lowest energies, where the single-crystal spectrometer was used. For the higher neutron energies, corrections were made for neutron effects, whereas we positively eliminated neutron effects over the entire energy region by time of flight. The effect of their corrections is discussed further two paragraphs below.

No time-of-flight separation whatsoever was used in the work of Rau[24] who reported a rather high value of 9.5 ± 0.2 MeV/fission in 1963. This is 3 MeV above our value, with combined error of only 0.5 MeV. Their data were for 0.1–2.5 MeV photons at 0–220 nsec after fission, and yield a value of $E_{\gamma,\,av} = 1.20$ MeV/photon. The delayed γ rays emitted between 10 and 220 nsec after fission can account for no more than ~0.1 MeV/fission, at most.[3] In addition to difficulties with neutron effects, sophisticated spectrum-unscrambling methods were not available at the time of their measurements.

Pleasonton, Ferguson, and Schmitt[25] have just recently measured $E_{\gamma,\,tot}$ and $E_{\gamma,\,av}$ as a function of fission-fragment mass by obtaining these quantities indirectly from the γ-ray pulse-height distribution with the use of a "weighting method" of Maier-Liebnitz. They did not obtain the energy spectrum in this way. Their values of $E_{\gamma,\,tot} = 6.43 \pm 0.3$ MeV/fission and $E_{\gamma,\,av} = 0.99$ MeV/photon were obtained for 0.09–10-MeV photons with an over-all time resolution of 5.3 nsec. They measured γ rays emitted at 0 and 180° with respect to the direction of the fission fragments. To obtain the value of $E_{\gamma,\,tot}$ averaged over all angles, they estimated that their results should be reduced by ~6%, yielding a value of ~6.06 MeV/fission. Their results then compare with our values of 6.51 ± 0.3 MeV/fission and 0.97 MeV/photon for 0.14–10-MeV photons at 0–10 nsec after fission, and for a time resolution of <4 nsec. For a direct comparison with our date, their result should be decreased by ~0.07 MeV/fission because of the difference in the lower energy limit, leaving a difference of

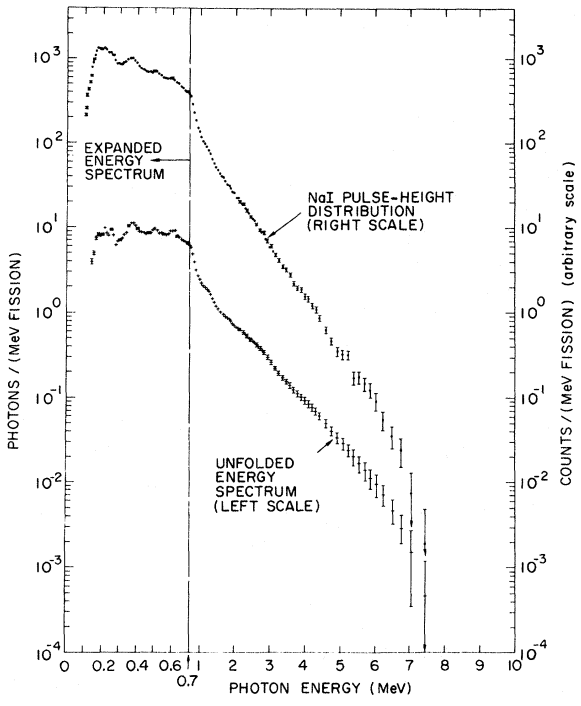

FIG. 8. NaI pulse-height distribution for prompt γ rays from the spontaneous fission of ^{252}Cf. Also shown is the unfolded spectrum. The error bars are too small to show in the 0.7- to 2-MeV region.

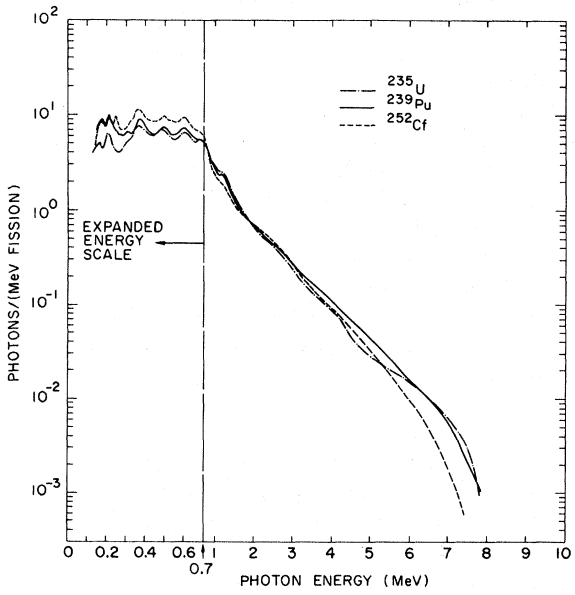

FIG. 9. Unfolded prompt γ-ray energy spectra for the thermal-neutron fission of ^{235}U and ^{239}Pu and for the spontaneous fission of ^{252}Cf. The error bars on the unfolded data are indicated in Figs. 6–8.

TABLE I. Energy emitted per fission in the form of prompt γ rays and the number of γ rays per fission for various γ-ray energy intervals. The uncertainties given in the table include only the statistical uncertainties and those due to unfolding. The relative values for the total energy per fission, $E_{\gamma,\mathrm{tot}}$, above 0.14 MeV for ^{235}U, ^{239}Pu, and ^{252}Cf, are known to an accuracy of about 0.1 MeV/fission, while the over-all error in absolute yield from 0.14 to 10 MeV is estimated to be 0.3 MeV for $E_{\gamma,\mathrm{tot}}$, including systematic errors.

Photon energy range (MeV)	Protons/Fission			MeV/Fission		
	^{235}U	^{239}Pu	^{252}Cf	^{235}U	^{239}Pu	^{252}Cf
0.14–0.3	0.833	1.267	1.270	0.181±0.005	0.275±0.007	0.282 ±0.007
0.3–0.5	1.318	1.473	1.855	0.532±0.013	0.596±0.015	0.759 ±0.019
0.5–0.7	1.182	1.219	1.613	0.709±0.028	0.737±0.019	0.963 ±0.024
0.7–1.0	1.191	1.097	1.067	1.021±0.026	0.939±0.023	0.908 ±0.023
1.0–1.5	1.072	0.998	0.838	1.337±0.034	1.241±0.031	1.044 ±0.026
1.5–2.0	0.461	0.450	0.442	0.804±0.020	0.787±0.020	0.778 ±0.020
2.0–2.5	0.258	0.268	0.292	0.582±0.015	0.606±0.015	0.660 ±0.017
2.5–3.0	0.158	0.175	0.183	0.434±0.012	0.482±0.014	0.503 ±0.013
3.0–4.0	0.143	0.173	0.160	0.490±0.015	0.597±0.017	0.550 ±0.014
4.0–5.0	0.050	0.0714	0.058	0.220±0.015	0.318±0.019	0.254 ±0.010
5.0–6.0	0.021	0.0265	0.019	0.116±0.011	0.145±0.018	0.102 ±0.009
6.0–7.0	0.0098	0.0104	0.0057	0.064±0.015	0.067±0.012	0.038 ±0.005
7.0–10.0	0.0027	0.0015	0.0004	0.019±0.015	0.019±0.012	0.0019±0.0014
0.14–10.0	6.70	7.23	7.80	6.51	6.81	6.84

0.52 MeV with combined errors of 0.6 MeV. This is reasonably good considering the differences in experimental methods. They used time-of-flight separation of neutrons from γ rays, after having first obtained some preliminary results[26] without time-of-flight separation. Since these preliminary results gave an appreciably higher value of $E_{\gamma,\mathrm{tot}}$ they state[25] that this suggests the experiments of Peelle and Maienschein[5] "may also have included detection of some neutrons, in spite of the precautions taken to exclude them."

The lower value obtained by Pleasonton, Ferguson, and Schmitt as compared to our data cannot be explained by inelastic scattering of the prompt fission neutrons by the thicker ^{235}U foil and stainless-steel backing in our arrangement, as these contribute a calculated upper limit of only about 0.0002 MeV/fission. The nearby fission-fragment detector and surrounding structural material viewed by the NaI detector can contribute no more than about 0.05 MeV/fission. Also, the steady-state backgrounds, and the near-steady-state backgrounds such as delayed neutrons from fission and neutron captures, were accurately removed in our background measurements, as described in Sec. II.

Measurements have been made for prompt γ rays from ^{252}Cf by Smith, Fields, and Friedman[27] and also by Bowman and Thompson.[28] In both cases, the accuracy was limited by the γ-ray spectrometry techniques at the time, including the lack of accurate pulse-height unfolding codes, and by prompt-fission-neutron interactions with the spectrometer. This probably accounts for values of $E_{\gamma,\mathrm{tot}}$ of 8.2 and 9.0 MeV/fission for the two respective experimental groups; these values are much higher than the value of 6.84 MeV/fission reported in this paper for ^{252}Cf.

VI. DISCUSSION OF RESULTS

In this section the present data are compared to related theoretical predictions of $E_{\gamma,\mathrm{tot}}$, the average photon energy $E_{\gamma,\mathrm{tot}}$, and the photon spectrum $\bar{\varphi}(E_\gamma)$ for ^{235}U thermal-neutron fission. In addition, a comparison between the experimental results for ^{235}U(n,f), ^{239}Pu(n,f), and ^{252}Cf(s.f.) is given along with some theoretical implications.

A. Comparison of ^{235}U Results with Theory

To the present experimental results of $E_{\gamma,\mathrm{tot}}$ 6.51 MeV/fission should be added ~4% to include photons below the 0.14-MeV low-energy cutoff[25] and all pre-β-decay photons emitted after the 0–10-nsec time interval of the measurement.[3-5] This yields a value of 6.77±0.4 MeV/fission.

As mentioned in the introduction, the earliest calculational results[6-9] are consistent with the picture that, following the neutron evaporation cascade, each of the two fission fragments is left with an excitation energy, emitted as photons, of about half the binding energy for emitting the next neutron, or $E_{\gamma,\mathrm{tot}} \simeq \bar{E}_b \leq 5$ MeV. This is roughly 2 MeV less than the experimental results. It is there-

fore evident that the early calculations require the addition of other effects that further inhibit the neutron emission that is in competition with γ-ray deexcitation of the fission fragments. The statistical theory calculation of Zommer, Saveliev, and Prokofiev[1] was more comprehensive, in that they took into account the possibility of γ-ray emissions preceding the emission of the last neutron. With their estimated values of $\overline{E}_b$, they obtained $E_{\gamma,\,tot}=6.2$ MeV/fission, which included 0.3 MeV as pre-neutron-emission photons. This upper limit would be nearer the experimental value of 6.77 MeV/fission if, as they stated, the calculation could have taken into account the large nuclear level spacing near ground state and the angular momentum barrier of the fission fragments to neutron emission.

The calculations of Gordon and Aras[10] included an explicit pairing-energy correction δ for level densities as mentioned in the introduction. They have assumed apparently too great a neutron-emission barrier in that their results of $E_{\gamma,\,tot}\cong\overline{E}_b+\delta$ $=7.66$ MeV is nearly 1 MeV too high. For $\delta=0$, they obtain $E_{\gamma,\,tot}=5.03$ MeV, or a difference of 2.63 MeV. It is interesting to note that if they had reduced the effect of δ by ~2/3, their calculation would have lead to agreement with the experiment reported here. This strongly suggests that their assumption of no neutron emission for fission-fragment excitation energies below $(\overline{E}_b+\delta)$ is too severe.

The calculations of Thomas and Grover[12] do not predict $E_{\gamma,\,tot}$ directly, but using a measured value of $E_{\gamma,\,tot}$ plus the binding and kinetic energies of the cascade neutrons they first calculate the average total fission-fragment initial excitation energy $\overline{E}^*$. Using this value of $\overline{E}^*$, they predict the partition of deexcitation energy between neutron and photon emission. This was done only for the "average" light fission fragment, ^{96}Sr, and the complementary heavy fragment, ^{140}Xe. In their original calculations Thomas and Grover assumed a value of 7.5 MeV/fission for $E_{\gamma,\,tot}$ in order to determine the initial fission-fragment excitation energy. The predicted value of $E_{\gamma,\,tot}$ for the 140/96 mass split is then 7.1 MeV/fission, which is 0.4 MeV below the value of $E_{\gamma,\,tot}$ used as input to the calculation. This indicates that the calculation is somewhat incorrect or that the wrong initial value was used for $E_{\gamma,\,tot}$. We found that a more up to date value for $E_{\gamma,\,tot}$ as input gives better agreement. We recalculated $E_{\gamma,\,tot}$, using $6.77+0.3$ MeV/fission as the energy emitted by γ-ray emission, because experimental evidence[26] yields 0.3 MeV more energy for the 140/96 mass split than for $E_{\gamma,\,tot}$ averaged over all fission fragments. We also used the Grover and Thomas values for E_b(light), E_b(heavy), and $\overline{E}_n$ (kinetic energy). With these inputs, we obtained a predicted value of 6.9 MeV/fission for $E_{\gamma,\,tot}$, and 0.86 MeV/photon for $E_{\gamma,\,av}$. The predicted value of 6.9 MeV, after being reduced by 0.3 MeV, yields 6.6 MeV which agrees well with our estimated value of $6.5\times1.04=6.77\pm0.4$ MeV fission for all γ rays preceding β-ray emission. The present experimental value of $E_{\gamma,\,av}=0.97\pm0.05$ MeV is in fair qualitative agreement with the value of 0.86 MeV/photon predicted by Thomas and Grover, considering that the present value does not include photons below the 0.14-MeV cutoff of the measurement and the relatively low-energy photons emitted later than 10 nsec after fission.[3] This predicted value is still somewhat low, as can be seen in a comparison of the measured and calculated spectra presented below. Nevertheless, the present measurements are in reasonably good support of their calculations, and of the preceding work by Grover and Nagle[11] on which the spin barrier to neutron emission was based. This work[11] was discussed in the introductory remarks of this report.

The calculations of Thomas and Grover can be used to predict $E_{\gamma,\,tot}$ as a function of neutron bombarding energy. The predicted values of $E_{\gamma,\,tot}$ contributed by each fission fragment, when plotted

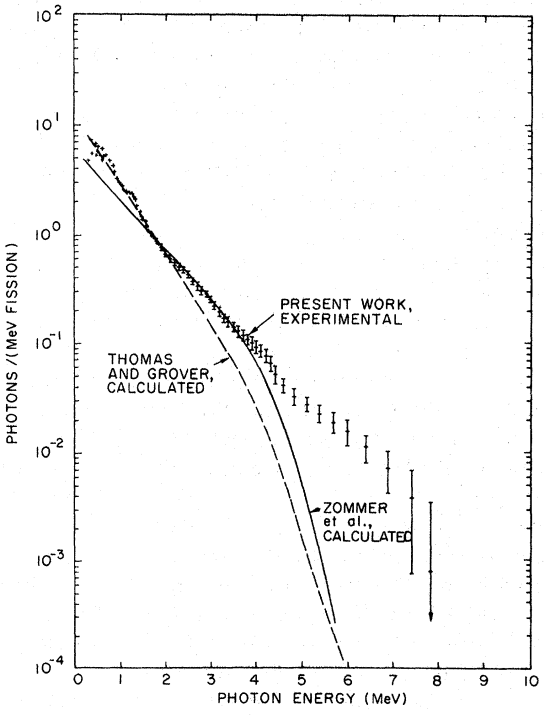

FIG. 10. Present experimental results for $^{235}U(n,f)$ compared to the calculations of Zommer, Saveliev, and Prokofiev (Ref. 1) and of Thomas and Grover (Refs. 12 and 13). The theoretical curves were slightly normalized (<10%) to the measured results.

against the initial excitation energy $\bar{E}^*$ of each fragment, show a slow rise with $\bar{E}^*$ superposed on an oscillation with a period of $\bar{E}_b$ for the given fragment.[12] Values of about 9.5 and 8.0 MeV for $E_{\gamma,\,\mathrm{tot}}$ are predicted at neutron bombarding energies E_n of 12 and 14 MeV, respectively. An iterative calculation was utilized, adjusting $\bar{E}^*$ so that the total energy was conserved. The energy taken off by neutrons was calculated from the known values of the prompt-neutron yield, ν_p, versus neutron bombarding energy. The partition of neutrons emitted per fragment and initial excitation energy per fragment were taken as constant with E_n. Calculation of the average kinetic energy of the cascade neutrons was carried out with prescriptions cited in the Grover and Thomas reference.[12] Values of $\bar{E}_b$ were obtained from a simple straight line extrapolation between the values given for the ^{96}Sr and ^{140}Xe cases. It would be of interest to compare the above predictions to experiments carried out at a number of neutron energies.

A prediction of the γ-ray spectrum for ^{235}U(n,f) was obtained from the calculation of Thomas and Grover,[12] but was not published. This spectrum was graciously made available to us by J. R. Grover.[13] It is shown in Fig. 10, along with that of Zommer, Saveliev, and Prokofiev[1] and the present experimental results. The spectrum of Thomas and Grover fits the data well below 2 MeV, where over 0.7 of $E_{\gamma,\,\mathrm{tot}}$ and over 0.9 of the total number of photons are found.

The spectral prediction of Zommer, Saveliev, and Prokofiev[1] on the other hand, is in better agreement with the measured spectrum at higher energies. The two agree especially well between 1.5 and 4 MeV.

B. Intercomparison of ^{235}U(n,f), ^{239}Pu(n,f), and ^{252}Cf(s.f.) Results

The three γ-ray spectra shown in Fig. 9 have nearly the same over-all shape, and have nearly all the γ-ray peaks below 2 MeV in common. Table I gives values of 6.51, 6.81, and 6.84 MeV/fission for $E_{\gamma,\,\mathrm{tot}}$ and 6.70, 7.23, and 7.80 photons per fission for ^{235}U(n,f), ^{239}Pu(n,f), and ^{252}Cf(s.f.), respectively, for energies greater than 140 keV and for 0–10 nsec after fission. There is no definite tendency for $E_{\gamma,\,\mathrm{tot}}$ to increase with the mass of the fissionable nucleus, although the softness of the spectrum, as represented by $E_{\gamma,\,\mathrm{av}} = E_{\gamma,\,\mathrm{tot}}/$(photons/fission), does show a clear decrease with mass.

It is interesting to speculate briefly on the possible effects of the initial spin on $E_{\gamma,\,\mathrm{tot}}$, since the initial spin of ^{235}U is $\frac{7}{2}$ and that for ^{239}Pu is $\frac{1}{2}$. If a higher initial spin of the pre-fission nucleus were to imply a higher initial spin for each of the two fission fragments, on the average, then one would expect to have a higher barrier for neutron emission from ^{235}U than from ^{239}Pu. However, ^{235}U exhibits a smaller value of $E_{\gamma,\,\mathrm{tot}}$ than ^{239}Pu. These data indicate there is little correlation between the spin of the pre-fission nucleus and the average spin of the fission fragment. This conclusion is apparently not affected by the change in the mass or the fissionability parameter Z^2/A between ^{235}U and ^{239}Pu. The change in $E_{\gamma,\,\mathrm{tot}}$ with these parameters is small as indicated by our identical values of $E_{\gamma,\,\mathrm{tot}}$ for ^{239}Pu and ^{252}Cf.

C. Level-Density Arguments for Differences in $E_{\gamma,\,\mathrm{av}}$

The difference in the shapes of the γ-ray spectra, as reflected in the $E_{\gamma,\,\mathrm{av}}$ values of 0.97, 0.94, and 0.88 MeV/photon above 0.14 MeV for ^{235}U, ^{239}Pu, and ^{252}Cf, respectively, show a much stronger dependence on mass than did the values of $E_{\gamma,\,\mathrm{tot}}$, and may possibly be explained by the following arguments. The softer γ-ray spectrum for ^{252}Cf is probably related to the higher average level density of the fission fragments for this case, or possibly to the nature of the levels, and the manner in which these parameters vary with the mass of the fission fragments. In a study of K x-ray yields as a function of fission-fragment mass, Wehring and Wyman[29] found that for ^{235}U(n,f), the K x-ray yield was large only at the upper end of the light-fragment peak (at $Z = 40$–42) of the fission-fragment mass-yield curve. This is consistent with a higher level density at this high-mass end of the low-mass peak, and is a result of these nuclei being located within the edge of the region where deformed nuclei are found. The higher level density increases the probability of internal conversion, and thus increases the probability of K x-rays. These x-ray measurements, in fact, help define the boundary of the distorted-nucleus region. For ^{252}Cf, the light-mass peak completely straddles the region of distorted nuclei, according to Fig. 12 of Glendenin and Unik,[30] so that nearly all of the light-fragment yield falls in this region. This is consistent with the x-ray yields observed for ^{252}Cf by Glendenin and Unik[30] and Kapoor, Bowman, and Thompson.[31] At the heavy-mass peak of the mass-yield curve, the same argument holds. For ^{252}Cf, the upper end of the heavy-fragment mass-yield peak is further into the distorted-nucleus region, since it is further from the $Z = 50$, $N = 82$ stability lines. For ^{239}Pu, both the upper and lower peaks of the mass-yield curve lie between the corresponding peaks for ^{235}U and ^{252}Cf, but nearer to the ^{235}U peaks. This is consistent with the relative values of $E_{\gamma,\,\mathrm{av}}$.

In addition to the greater level density in the distorted-nucleus region, as mentioned above, the presence of rotational spectra in this region may provide a series of levels through which the excited nucleus may become preferentially deexcited through a large over-all change in nuclear spin. Since the level spacing for rotational spectra is typically small, this type of deexcitation would be consistent with the observation of a smaller value of $E_{\gamma,\,av}$ for ^{252}Cf.

ACKNOWLEDGMENTS

The authors wish to express their gratitude to C. S. Young of the Los Alamos Scientific Laboratory (LASL) for making the LSMUN code available, to F. K. Smith and J. G. Povelites of LASL for fabrication and loan of the ^{239}Pu and ^{235}U foils, to C. Hohenemser of Brandeis University and W. A. Gibson of Tennecomp for suggestions regarding fast timing, to W. Whittemore and the TRIGA operating staff for help with the thermal-neutron beam, to L. A. Kull, C. E. Creutz, and E. Beaver for help with the early calculations, to W. John of the Lawrence Radiation Laboratory, J. R. Grover of the Brookhaven National Laboratory, J. J. Griffin of the University of Maryland, C. S. Young and F. K. Smith of LASL for helpful discussions, to C. A. Preskitt and J. R. Beyster for continued interest, encouragement, and helpful discussions.

---

†Work supported by Defense Nuclear Agency under contract DASA 01-69-C-0059.

[1]V. P. Zommer, A. E. Saveliev, and A. I. Prokofiev, At. Energ. 19(No.2) 116 (1965) [transl.: Soviet J. At. Energy 19, 1004 (1965)].

[2]S. A. E. Johansson, Nucl. Phys. 60, 378 (1964).

[3]V. V. Verbinski, H. Weber, and R. E. Sund, Trans. Am. Nucl. Soc. 14, 391 (1971); Gulf Report No. Gulf-RT-A10782; and to be published.

[4]R. B. Walton and R. E. Sund, Phys. Rev. 178, 1894 (1969).

[5]R. W. Peele and F. C. Maienschein, Phys. Rev. C 3, 373 (1971).

[6]R. B. Leachman, Phys. Rev. 101, 1005 (1956).

[7]R. B. Leachman and C. S. Kazek, Jr., Phys. Rev. 105, 1511 (1957).

[8]J. Terrell, Phys. Rev. 113, 527 (1959).

[9]J. Terrell, Phys. Rev. 108, 783 (1957).

[10]G. E. Gordon and N. K. Aras, in *Proceedings of the Symposium on the Physics and Chemistry of Fission, Salzburg, 1965* (International Atomic Energy Agency, Vienna, Austria, 1965), Vol. II, p. 73.

[11]J. R. Grover and R. J. Nagle, Phys. Rev. 134, B1248 (1964).

[12]J. R. Grover, Phys. Rev. 123, 267 (1962); T. D. Thomas and J. R. Grover, Phys. Rev. 159, 980 (1967).

[13]J. R. Grover, private communication.

[14]M. Hoffman, Phys. Rev. 133, B714 (1964).

[15]M. V. Blinov *et al.*, Zh. Eksperim. i Teor. Fiz. 43, 1644 (1962) [transl.: Soviet Phys. – JETP 16, 1159 (1963)].

[16]C. Hohenemser, Brandeis University, private communication.

[17]The National Bureau of Standards, Los Alamos Scientific Laboratory, New England Nuclear Corporation, and Centre à l'Energie Atomique (France).

[18]L. Jarczyk *et al.*, Nucl. Instr. Methods 17, 310 (1962).

[19]C. S. Young, Trans. Am. Nucl. Soc. 14, 388 (1971).

[20]B. C. Cook, Nucl. Instr. Methods 24, 256 (1963).

[21]B. Brunfelter, J. Kockum, and H. O. Zetterström, Nucl. Instr. Math. 40, 84 (1965).

[22]F. C. Maienschein, R. W. Peelle, W. Zobel, and T. A. Love, in *Proceedings of the Second United Nations International Conference on the Peaceful Uses of Atomic Energy* (United Nations, Geneva, Switzerland, 1958), Vol. 15, p. 366.

[23]V. V. Verbinski, R. E. Sund, and H. Weber, Defense Atomic Support Agency Report No. DASA-2234 (GA-9148) 5 April 1969 (unpublished).

[24]V. F. E. W. Rau, Ann. Physik 10, 252 (1963).

[25]F. Pleasonton, R. L. Ferguson, and H. W. Schmitt, Phys. Rev. C 6, 1023 (1972).

[26]F. Pleasonton, ORNL Report No. ORNL-TM-3205, 1970 (unpublished), p. 14.

[27]A. B. Smith, P. R. Fields, and A. M. Friedman, Phys. Rev. 104, 699 (1956).

[28]H. R. Bowman and S. G. Thompson, in *Proceedings of the Second United Nations International Conference on the Peaceful Uses of Atomic Energy* (see Ref. 22), Vol. 15, p. 212.

[29]B. W. Wehring and M. E. Wyman, Phys. Rev. 157, 1083 (1967).

[30]L. E. Glendenin and J. P. Unik, Phys. Rev. 140, B1301 (1965).

[31]S. S. Kapoor, H. R. Bowman, and S. G. Thompson, Phys. Rev. 140, 963 (1966).